Bridging Hydroxyl Groups in Faujasite: Periodic vs Cluster Density Functional Calculations

Jörg-Rüdiger Hill,*,† Clive M. Freeman,† and Bernard Delley‡

Molecular Simulations Inc., 9685 Scranton Road, San Diego, California 92121-3752, and Paul Scherrer Institut, Badenerstrasse 569, CH-8048 Zürich, Switzerland

Received: January 4, 1999; In Final Form: March 1, 1999

Periodic density functional calculations (DFT) on bridging hydroxyl groups in the zeolite faujasite are performed. It is shown that force field calculations as presently parametrized are not able to reproduce the correct energetical ordering for these groups. Embedding not only gives the right ordering but also agrees well with the periodic calculations for geometries. OH stretching frequencies can be obtained in very good agreement with experiment by periodic DFT calculations in particular if anharmonic corrections are included. The same functionals used for the periodic calculations have been employed in calculations on model clusters, and it is shown that clusters provide a qualitative as opposed to a quantitative description of these systems.

1. Introduction

Zeolites are microporous aluminosilicates with diverse properties that make them valuable as catalysts in a variety of technologically important processes. One key attribute is their Brønsted acidity which is caused by so-called bridging hydroxyl groups. A bridging hydroxyl group is formally formed by replacing a silicon atom in the zeolite framework with an aluminum atom.[1] To keep the system electrically neutral, an additional positive charge is required which can be provided by a proton. The proton can be attached to one of the oxygen atoms surrounding the aluminum atom thereby forming a bridging hydroxyl group. Bridging hydroxyl groups are difficult to observe experimentally since their concentration in a zeolite and their scattering power for X-rays are low. However, experimental information on bridging hydroxyl groups has been obtained by IR and NMR spectroscopy[2−5] as well as by neutron powder diffraction.[5,6] Furthermore, bond strengths, and therefore relative acidities, can be determined using vibrational spectroscopy with probe molecules (ref 7 and references therein).

Detailed information has been gained from theoretical calculations. These calculations, however, face some difficulties on their own. All industrial important zeolites have unit cells with hundreds of atoms. Therefore, most quantum mechanical calculations have used only cluster models which do not account for the effect of the lattice on the bridging hydroxyl group. Periodic lattice calculations on faujasite have been performed using force fields[8−10] or hybrid quantum mechanics/molecular mechanics embedding schemes.[11] For these methods to work reliably, force field parameters are required. Very recently periodic density functional calculations have become feasible for zeolites,[12−28] but the faujasite unit cell is so large that only the all-silica form has been investigated so far.[28] We report here on a study of bridging hydroxyl groups in faujasite using periodic density functional calculations. This study serves two purposes. Comparison of the results obtained from periodic calculations with results from cluster calculations using the same quantum mechanical method permits an assessment of the accuracy obtained in cluster calculations. We can also compare the results of periodic density functional calculations with the results of periodic embedding calculations and therefore validate this new approach.

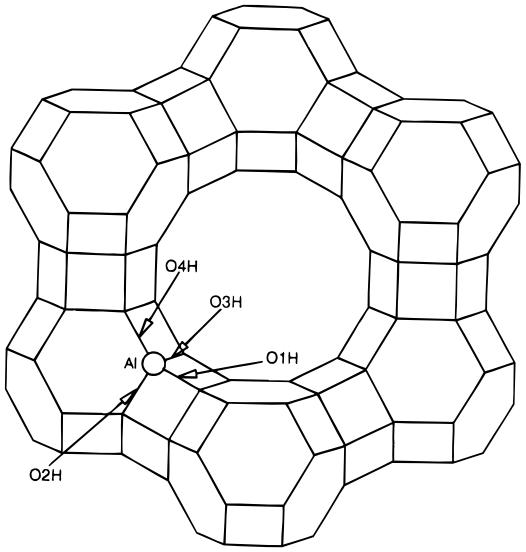

Figure 1. Four different sites a bridging hydroxyl group can be formed at in faujasite.

2. Calculations

The zeolite faujasite was chosen because it has only four crystallographically distinct oxygen atom sites and, in the form of zeolite Y and various derivatives, is an industrial important catalyst. Moreover, it has been studied thoroughly both experimentally and theoretically. Faujasite has a unit cell with $Fd\bar{3}m$ symmetry containing 576 atoms.[5] It is, however, possible to define a smaller rhombohedral cell with only 144 atoms. In our calculations we have used this smaller cell. One of the 48 silicon atoms in this cell was replaced by an aluminum atom, and a hydrogen atom was attached to one of the oxygen atoms bonded

* To whom correspondence should be addressed. Tel: (619) 799-5508. Fax: (619) 458-0136. E-mail: jxh@msi.com.
† Molecular Simulations Inc.
‡ Paul Scherrer Institut.

10.1021/jp990031k CCC: $18.00
Published on Web 04/22/1999

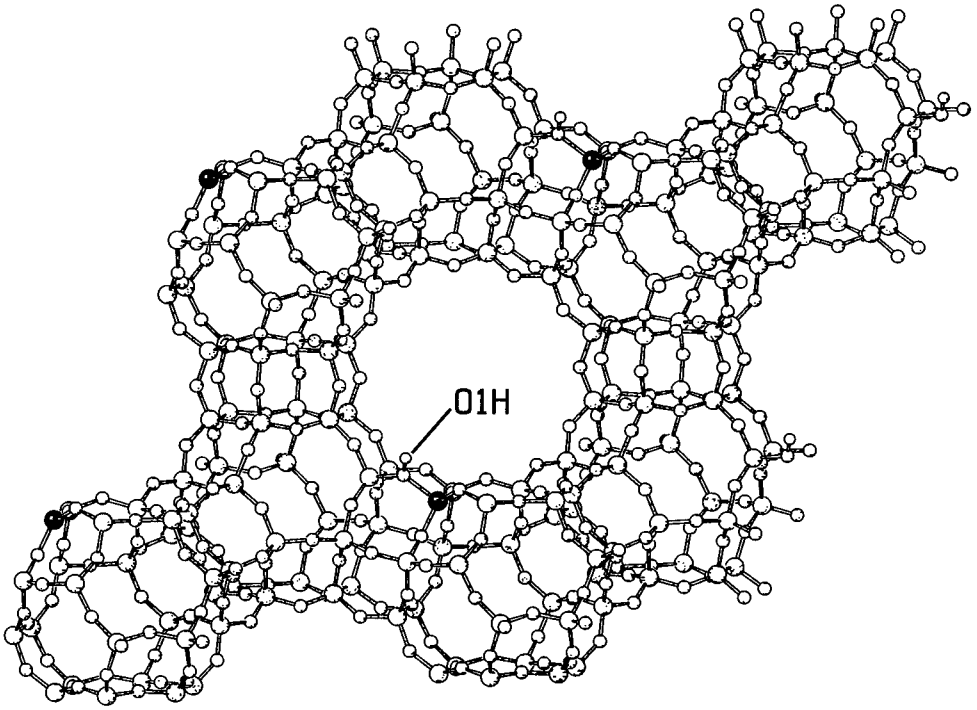

Figure 2. Bridging hydroxyl group at O1H as optimized using the VWN functional. The cell shown has been obtained from the cell used in the calculation by doubling *a* and *c*. The aluminum atom is the dark circle.

TABLE 1: Unit Cell Dimensions Obtained from Shell Model Structure Optimizations and Used in the Periodic DFT Calculations (pm and deg, Respectively)

	a	*b*	*c*	α	*β*	*γ*
O1H	1749	1745	1743	60.1	59.9	60.1
O2H	1747	1744	1745	60.0	60.1	60.2
O3H	1743	1744	1744	60.1	60.1	60.3
O4H	1747	1746	1745	59.9	60.0	60.0

directly to the aluminum atom. There are four distinct bridging configurations; the resulting structures will be named O1H and O4H according to the usual naming convention for the oxygen atoms in faujasite[29] (cf. Figure 1). The resulting structures were geometry optimized using Sierka and Sauer's density functional based shell model potential.[10] During this optimization the unit cell was allowed to relax. The unit cell dimensions obtained are shown in Table 1. Starting from the shell model potential optimized structures, full geometry optimizations were performed for all four systems using the local density functional of Vosko−Wilk−Nusair (VWN)[30] with a double numerical basis set with polarization functions (DNP) and a "medium" grid corresponding to $14(Z + 2)^{1/3}$ shells per atom for the radial part (Z − atomic number) up to 10 atomic units from the nucleus and the number of angular points chosen (up to a maximum of 194) such that the precision of the integration was 10^{-4} atomic units.[31,32] During this optimization the unit cell was kept fixed. The structures were considered to be converged when the change in energy between two iterations was smaller than 10^{-5} hartree and gradient and displacement were less than 10^{-3} hartree ${a_0}^{-1}$ and 10^{-3} a_0, respectively. Between 37 and 50 iterations were required to reach convergence. Figure 2 shows the structure obtained for O1H. All calculations were performed using DMol[3] [33] on a single node of an IBM SP2. Single-point energies were calculated for the VWN optimized structures using the gradient-corrected density functional of Perdew and Wang (GGA).[34,35]

The OH stretch frequency was determined for the optimized structures by numerical differentiation. For this purpose four energies were calculated with the OH bond stretched by ±0.03 a_0 (= x) and ±0.06 a_0 (= y). The harmonic force constant, F_{ii}, was obtained according to

$$F_{ii} = \frac{V(x) + V(-x) - V(y) - V(-y)}{x^2 - y^2} \tag{1}$$

and used to determine the wave number, $\bar{\nu}$,

$$\bar{\nu} = \sqrt{GF_{ii}}/2\pi c \tag{2}$$

where $G = m_O^{-1} + m_H^{-1}$ and c is the speed of light. Anharmonicity constants were calculated using the cubic force constants and assuming a Morse potential, since the calculation of quartic force constants from the energies proved to be numerically too unstable as shown below. Cubic force constants, F_{iii}, were obtained from

$$F_{iii} = 3\frac{V(x) - V(-x) + V(y) - V(-y)}{x^3 + y^3} \tag{3}$$

which gives the anharmonicity constant, x_{OH}, for a Morse potential

$$x_{OH} = \frac{\hbar G}{72\pi^2 c}\frac{F_{iii}^2}{F_{ii}} \tag{4}$$

where $\hbar$ is Planck's constant. Considering the error in the integration—and therefore in the energies—of $\pm 10^{-4}$ hartrees, error propagation can be used to estimate the error in the force constants obtained by numerical differentiation. For the harmonic force constants, an error of ±200 N m^{-1} is obtained (20% of a typical harmonic OH stretch force constant) while for the cubic force constant the error is $\pm 1.6 \times 10^{13}$ N m^{-2} (25% of a typical cubic OH stretch force constant). The quartic force constant would have to be obtained from two harmonic force constants (cf. ref 36) which boosts the error to $\pm 1.4 \times 10^{27}$ N

TABLE 2: Relative Energies of the Four Bridging OH Groups in H−Faujasite (kJ/mol)

	O1H	O2H	O3H	O4H
empirical shell model potential[8]	0.0	14.5	−5.3	18.4
ab initio shell model potential[9]	0.0	9.2	−8.8	19.1
DFT shell model potential[10]	0.0	6.0	−11.1	13.6
embedded cluster[11]	0.0	28.7	4.6	22.6
periodic DFT/VWN/DNP//DFT/VWN/DNP	0.0	10.8	3.4	8.6
periodic DFT/GGA/DNP//DFT/VWN/DNP	0.0	9.8	4.9	7.9

TABLE 3: Uncoupled and Unscaled OH Stretching Frequencies of the Four Bridging OH Groups in H−Faujasite as Well as Calculated Anharmonicity Constants (cm^{-1})

	O1H	O2H	O3H	O4H
Harmonic OH Stretching Frequencies				
empirical shell model potential[8]	3772	3702	3736	3751
DFT shell model potential[10]	3723	3602	3644	3673
embedded cluster[11]	4003	3897	3872	3989
DFT/VWN/DNP	3731	3645	3606	3706
obsvd[45]	3787		3707	
Anharmonic OH Stretching Frequencies				
anharmonicity constant, DFT/VWN/DNP	−67.6	−59.4	−24.2	−62.7
anharmonic frequency, DFT/VWN/DNP	3596	3526	3558	3581
obsvd[2]	3623		3550	

m^{-3} (or more than 30 000% of a typical quartic OH stretch force constant, cf. ref 36) and explains the numerical instability observed. Increasing the size of the grid in the numerical integration would not be of much help since even the maximum grid size available in DMol[3] yields at most $\pm 10^{-6}$ hartrees and therefore an error of $\pm 1.4 \times 10^{25}$ N m^{-3} for the quartic force constant. Therefore, anharmonicity constants could only be calculated assuming a Morse potential. Experimental work indicates that a Morse potential is indeed a good approximation.[37]

The bridging hydroxyl groups at the different sites in faujasite are located either between two four-membered rings (O1H and O3H) or between a four-membered and a six-membered ring (O2H and O4H). In addition to the periodic calculations on faujasite we therefore performed cluster calculations on aluminum-cyclotetrasilicic acid (a model for a four-membered ring), $AlSi_3O_{12}H_9$, aluminum-cyclohexasilicic acid (a model for a six-membered ring), $AlSi_5O_{18}H_{13}$, aluminum-octahydroxy-silsesquioxane (a model for two fused four-membered rings), $AlSi_7O_{20}H_9$, and dialuminum-dodecahydroxy-silsesquioxane (a model for a four-membered ring fused with a six-membered ring), $Al_2Si_{10}O_{30}H_{14}$. The clusters were completely geometry optimized using both the VWN and GGA density functionals and the same basis set and grid as the periodic calculations. Hartree−Fock results for aluminum-cyclotetrasilicic and aluminum-cyclohexasilicic acid are available in the literature.[38]

3. Results and Discussion

Experimental studies on that system have revealed that only three of the four bridging OH groups are formed in nature.[6] The site occupations for O1H:O2H:O3H:O4H are 3:1:1.6:0 for a faujasite with the composition $Na_3H_{53}Al_{56}Si_{136}O_{384}$. Table 2 shows the relative energies for the four sites and compares them with results obtained previously by different methods. First, it is apparent that the sites O1H and O3H are significantly lower in energy than O2H and O4H regardless of the method used. Shell model potentials yield O3H to be the most stable site while embedding and periodic density functional calculations result in O1H to be lowest in energy. The energetical differences between the different sites are, in general, smaller in the periodic density functional calculations than in the other methods. Except for the shell model potentials all methods predict O4H to be lower in energy than O2H which suggests that the energetical stability of a particular site is not the only factor determining the experimental findings.

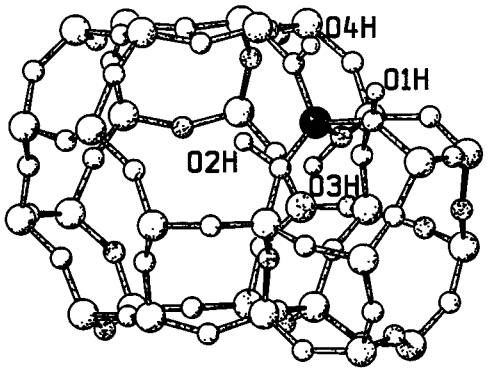

Figure 3. Bridging hydroxyl group at O3H points into the framework which causes its lower anharmonicity constant. The aluminum atom is the dark circle.

Table 3 compares the wavenumbers of the OH stretch mode obtained from different methods. This table also includes anharmonicity constants calculated as described in the previous section. Harmonic frequencies obtained for O1H and O3H show an error of less than 3% compared to the "observed" harmonic frequencies. Harmonic frequencies can, however, not directly be observed, they are calculated from the observed anharmonic frequencies using anharmonicity constants which are difficult to measure. A better comparison is therefore possible between calculated and observed anharmonic frequencies. If the harmonic frequencies are corrected for the anharmonicity of the OH stretching (which is only one part of the anharmonicity correction, but corrections for angle bending are supposed to be small, cf. ref 36), the error compared to the observed anharmonic frequencies is reduced to less than 0.75%. The so-called low-frequency mode corresponds to O3H while the high-frequency mode is caused by O1H. This assignment is the same as the one performed on the basis of force field calculations.

As a referee pointed out, the anharmonicity constant for hydroxyl groups has been found to be fairly constant in general. A comparison of the calculated anharmonicity constants shows, however, that this constant is much smaller for O3H than for the other three positions. This can be understood by looking at the local environment of the hydroxyl groups. O1H and O4H both point into a supercage and are therefore free to vibrate. O2H points into a six-membered ring, but this six-membered ring is part of the wall of a supercage. The hydroxyl group is therefore restricted only on one side. In contrast, in the O3H position the hydroxyl group points into the inside of one of the β- (or sodalite) cages and is surrounded by eight oxygen atoms at distances between 250 and 405 pm (cf. Figure 3). This restriction probably causes the lower anharmonicity constant.

Table 4 lists geometrical parameters of the bridging hydroxyl groups calculated by different methods. It is obvious that the lattice has a significant effect on the structure depending on the position of the bridging hydroxyl group. The SiO(H)Al angle, e.g., can vary by more than 11°. In general, there is good agreement between the structure of the bridging OH group obtained from periodic density functional (DFT) calculations and that resulting from embedding. Some larger differences can

TABLE 4: Selected Bond Lengths and Bond Angles Obtained for Bridging Hydroxyl Groups in Periodic Density Functional Calculations on Faujasite (pm and deg)

		O1H	O2H	O3H	O4H
r(SiO)	empirical shell model potential[8]	169.4	168.7	169.7	168.8
	ab initio shell model potential[9]	169.6	168.9	169.1	169.6
	DFT shell model potential[10,a]	170.7	169.6	169.3	170.5
	embedded cluster[11]	170.4	169.6	171.2	169.4
	DFT/VWN/DNP	170.5	169.9	170.5	170.1
r(AlO)	empirical shell model potential	191.0	190.3	193.0	190.6
	ab initio shell model potential	191.4	189.6	194.7	189.4
	DFT shell model potential	189.8	189.4	193.5	189.3
	embedded cluster	190.0	189.6	194.6	188.1
	DFT/VWN/DNP	190.9	190.5	192.1	190.6
r(OH)	empirical shell model potential	100.0	100.4	100.2	100.1
	ab initio shell model potential	95.4	96.9	96.1	96.1
	DFT shell model potential	97.0	98.5	97.9	97.8
	embedded cluster	95.6	96.2	96.2	95.8
	DFT/VWN/DFT	98.0	98.5	98.4	98.2
r(AlH)	empirical shell model potential	238.6	229.6	233.2	236.3
	ab initio shell model potential	247.6	234.7	239.7	241.6
	DFT shell model potential	246.0	237.0	240.2	241.4
	embedded cluster	247.8	237.9	246.8	242.4
	DFT/VWN/DFT	249.0	237.2	242.1	243.6
	obsvd[46]	248 ± 4		240 ± 4	
$\langle r(\mathrm{AlO})\rangle$	empirical shell model potential	173.8	174.3	174.2	174.3
	ab initio shell model potential	175.8	175.8	176.4	175.9
	DFT shell model potential	176.2	176.2	176.6	176.6
	embedded cluster	175.6	175.9	176.4	175.7
	DFT/VWN/DNP	176.0	176.2	176.1	176.3
∠SiO(H)Al	empirical shell model potential	131.1	142.4	138.7	134.0
	ab initio shell model potential	130.2	141.8	140.2	132.9
	DFT shell model potential	129.8	138.8	136.5	133.9
	embedded cluster	125.8	137.7	132.2	131.1
	DFT/VWN/DNP	128.7	140.4	136.1	134.2
	obsvd[6]	135.7	144.6	139.8	143.9
∠SiOH	empirical shell model potential	123.0	117.6	120.7	121.4
	ab initio shell model potential	114.5	111.9	113.8	112.7
	DFT shell model potential	116.0	113.9	117.1	114.1
	DFT/VWN/DNP	116.1	112.9	115.3	114.0

[a] Data for O1H and O3H from ref 10, the remaining from this work.

be found for the AlO bond lengths in O3H and O4H (2.5 pm), but otherwise both the AlO and SiO bond lengths differ by less than 1 pm. The OH bond lengths are slightly longer in the periodic DFT calculations compared to both the ab initio shell model potential and embedding calculations. However, it is known that the VWN functional overestimates these bonds lengths[39] and a shortening of the OH bond can be observed using gradient corrections in the cluster models (vide infra). The AlH distance which is known experimentally for O1H and O3H is predicted by the periodic DFT calculations well within the experimental error bars. The average AlO distance (averaged over all four AlO bonds per Al tetrahedron) is nearly constant for all different bridging hydroxyl group positions. The SiO(H)Al angle differs significantly for the different hydroxyl groups. In the observed structure, O1H and O3H have the smallest SiO(H)Al angle. All calculations predict O1H to have the smallest angle, but O3H and O4H switch positions. However, it should be noted that the observed structure has a much higher Al/Si ratio than the one used in the calculations and the bond angles observed are averaged over all possible sites. Since no proton could be observed on O4H that angle will necessarily be larger in experiment than in the calculation. Embedding systematically underestimates the SiO(H)Al angle compared to that in the periodic calculation.

Finally, Table 5 shows the charges for the bridging hydroxyl groups calculated according to Hirshfeld partioning.[40] Previous studies have often used Mulliken charges (e.g., ref 41). However, this method of partioning the electron density strongly depends on the basis set used and would not allow comparisons between calculations employing different basis sets.

TABLE 5: Hirshfeld Charges Calculated for the Four Different Bridging Hydroxyl Groups and Distances of Hydrogen Atom to Next Oxygen Atoms, DFT/VWN/DNP (e and pm)

	O1H	O2H	O3H	O4H
Si	0.5644	0.5672	0.5701	0.5603
O	−0.1689	−0.1680	−0.1745	−0.1631
H	0.2235	0.1993	0.1986	0.2220
Al	0.5010	0.5038	0.5148	0.4933
r(H···OSi)	260.0	249.4	257.7	253.8
r(H···OAl)	278.2	247.6	250.6	267.3

While the charges for the oxygen, silicon, and aluminum atom vary little between the different hydroxyl groups, the charge on the hydrogen atom is different between O1H and O4H on one side and O2H and O3H on the other side. This can be understood by considering the directions into which each OH group points. In O1H and O4H the OH group points into the supercage while in O2H and O3H it points into a six-membered ring. The distances between the hydrogen atom and the next oxygen atoms of the framework listed in Table 5 show that a larger positive charge on the hydrogen atom occurs if it is at a larger distance from these oxygen atoms.

Geometry optimizations of the cluster models proved difficult. The terminal hydroxyl groups formed intramolecular hydrogen bonds in all models but one, which completely distorted the structure of the aluminum-cyclotetrasilicic acid. Geometric results for this cluster model will therefore not be reported. This

TABLE 6: Selected Bond Lengths and Bond Angles Obtained for Bridging Hydroxyl Groups in Cluster Models (pm and deg)

model	functional	*r*(SiO)	*r*(AlO)	*r*(OH)	∠SiO(H)Al	∠SiOH(Al)
$AlSi_5O_{18}H_{13}$	VWN	168.5	191.7	97.9	137.9	112.9
$AlSi_5O_{18}H_{13}$	GGA	170.8	197.1	97.5	141.0	111.6
$AlSi_7O_{20}H_9$	VWN	168.3	189.9	98.1	129.5	119.1
$AlSi_7O_{20}H_9$	GGA	170.7	195.1	97.6	131.7	116.8
$Al_2Si_{10}O_{30}H_{14}$	VWN	167.9	189.9	98.3	136.4	117.6
$Al_2Si_{10}O_{30}H_{14}$	GGA	170.7	194.3	97.6	136.6	114.9

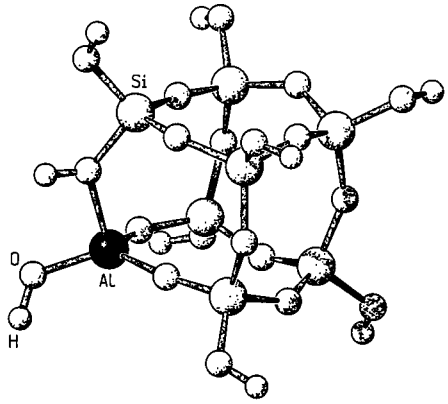

Figure 4. Structure of aluminum-octahydroxy-octasilsesquioxane as optimized using the VWN functional.

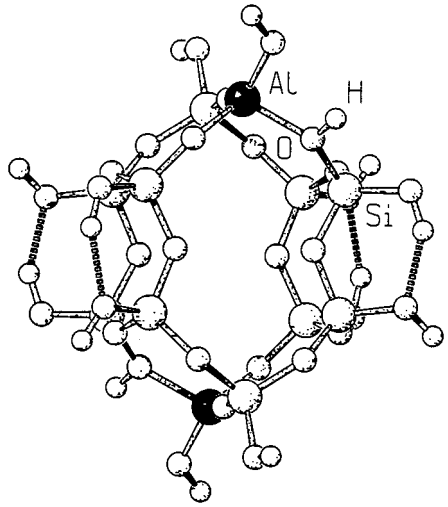

Figure 5. Structure of dialuminum-dodecahydroxy-dodecasilsesquioxane as optimized using the VWN functional. Some intramolecular hydrogen bonds are present.

unfortunate behavior of cluster models has been shown before.[1,42] Two of the other cluster models have some hydrogen bonds too, but the structure of the bridging hydroxyl group is not affected by them (cf. Figures 4 and 5). Previous Hartree−Fock calculations on cluster models have shown much less intramolecular hydrogen bonding[38] but used symmetry, and therefore they represent more geometrically constrained calculations. Due to the position of the bridging hydroxyl groups in our models, only C_s symmetry for aluminum-cyclohexasilicic acid and C_i symmetry for dialuminum-dodecahydroxy-silsesquioxane were employed in the present work. Bond lengths and bond angles for the bridging hydroxyl groups for the cluster models are shown in Table 6.

If we compare the geometries obtained with the local functional with those from the gradient-corrected functional, it is obvious that the AlO and SiO bonds are elongated using gradient corrections while the OH bond is shortened. It is known that the GGA functional used here tends to overestimate bond lengths in bonds involving second-row elements by on average around 3 pm.[39] The VWN functional also tends to overestimate these bond lengths, but only by around 2.5 pm. In our calculation, however, on average the AlO bonds become longer by 5 pm while the SiO bonds become longer by 2.5 pm. The OH bonds shorten by 0.5 pm on average which is the same magnitude as found by Scheiner et al. in their extensive study of the performance of different density functionals.[39]

It is also interesting to compare the structures obtained from the cluster models with the results of the periodic calculations. O1H and O3H are located between two four-membered rings and should therefore be compared with aluminum-octahydroxy-silsesquioxane. The SiO bond is 168.3 pm long in the cluster, but it is 170.5 pm in the periodic system. The AlO bond lengths and the SiO(H)Al angle agree well between cluster and O1H (189.9 vs 190.9 pm and 129.5° vs 128.7°, respectively) and show somewhat larger differences between cluster and O3H (189.9 vs 192.1 pm and 129.5° vs 136.1°, respectively). O2H and O4H are located between a six-membered ring and a four-membered ring and should therefore be compared with dialuminum-dodecahydroxy-silsesquioxane. Here, neither of the SiO bond lengths in the periodic system agrees with the cluster result (cluster: 167.9 pm; periodic: 169.9, 170.1 pm), but the AlO bonds are much closer in the cluster (189.9 pm) and periodic systems (190.5, 190.6 pm). The SiO(H)Al angle also differs considerably (cluster: 136.4°; periodic: 140.4, 134.2°). It is clear, therefore, that cluster calculations should be treated with care if they are supposed to mimic periodic systems.

If one looks at the Hirshfeld charges obtained for a bridging hydroxyl group, e.g., in dialuminum-dodecahydroxy-silsesquioxane (Si: 0.5336; O: −0.1668; H: 0.2080; Al: 0.4927), it is obvious that they are close to the charges obtained for the periodic calculations for O2H and O3H. However, the distances between the hydrogen atom and the next oxygen atoms in dialuminum-dodecahydroxy-silsesquioxane are shorter (r(H···OSi) = 266.1 pm, r(H···OAl) = 231.9 pm), and the hydrogen charge, therefore, is different from the charge obtained for O1H and O4H in the periodic calculation. On the other hand, for aluminum-cyclohexasilicic acid these distances are larger (r(H···OSi) = 283.5 pm, r(H···OAl) = 300.3 pm) and the hydrogen charge (0.2183 e) consequently is closer to the one obtained for O1H and O4H in the periodic calculations.

Some attempts have been made in the past to derive an "average" structure of a bridging hydroxyl group based on cluster calculations.[38,43,44] The most recent suggestion by Hill and Sauer[38] distinguishes between isolated and next nearest neighbor bridging hydroxyl groups. There is good agreement between their average value for the OH bond length of 96.6 ± 0.3 pm and the one predicted from our periodic calculations of 96.9 ± 0.3 pm. On the basis of our periodic calculations, the average SiO bond length is 168 ± 3 pm and the average AlO bond length 189 ± 3 pm. Our value for the SiO bond length falls into the range of 165.8−169.5 pm that Hill and Sauer predicted for isolated OH groups and also agrees with earlier suggestions of 168.5 pm by Sauer.[44] The situation is different for the AlO bond length. Hill and Sauer predicted 192.1−199.1 pm for isolated OH groups. Our value, however, agrees better

with the range of 187.9−190.4 pm they predicted for next nearest neighbor OH groups. The calculations Hill and Sauer used to arrive at their suggestions employed clusters with high Al/Si ratio. The need to accommodate several long AlO bonds in the cluster apparently puts strain on the AlO bonds in a manner analogous to the periodic system and leads to the observed bond shortening.

4. Conclusions

Empirical and ab initio shell model potentials yield energetical orderings for the bridging hydroxyl groups which differ from those obtained in embedding and periodic DFT calculations. Since O1H is found to have the highest occupation experimentally, in accord with periodic DFT and embedding results, it may be assumed that the ordering predicted by these methods is the correct one. The OH stretching frequencies obtained using periodic DFT calculations are in excellent agreement with experiment, in particular when anharmonic corrections are applied. The structure of bridging hydroxyl groups can be predicted by both embedding and periodic DFT calculations to the same accuracy. DFT calculations overestimate bond lengths, in particular bonds involving second-row elements. Local functionals, such as VWN, are more reliable for these bonds but tend to overestimate the OH bond lengths. The charge on the hydrogen atom in the bridging hydroxyl group depends on the distance of the hydrogen atom from the next framework oxygen atoms. Cluster calculations are of limited value in predicting quantitatively structures and charges of bridging hydroxyl groups.

References and Notes

(1) Sauer, J. In *Advances in molecular electronic structure theory*; JAI Press Inc.: 1994; Vol. 2, page 111.
(2) Anderson, M. W.; Klinowski, J. *Zeolites* **1986**, *6*, 455.
(3) Freude, D.; Klinowski, J.; Hamdan, H. *Chem. Phys. Lett.* **1988**, *149*, 355.
(4) Pfeifer, H.; Freude, D.; Hunger, M. *Zeolites* **1985**, *5*, 274.
(5) Hriljac, J. A.; Eddy, M. M.; Cheetham, A. K.; Donohue, J. A.; Ray, G. J. *J. Solid State Chem.* **1993**, *106*, 66.
(6) Czjzek, M.; Jobic, H.; Fitch, A. N.; Vogt, T. *J. Phys. Chem.* **1992**, *96*, 1535.
(7) Sauer, J.; Hill, J.-R. *Chem. Phys. Lett.* **1994**, *218*, 333.
(8) Schröder, K.-P.; Sauer, J.; Leslie, M.; Catlow, C. R. A.; Thomas, J. M. *Chem. Phys. Lett.* **1992**, *188*, 320.
(9) Schröder, K.-P.; Sauer, J. *J. Phys. Chem.* **1996**, *100*, 11043.
(10) Sierka, M.; Sauer, J. *Faraday Discuss.* **1997**, *106*, 41.
(11) Eichler, U.; Brändle, M.; Sauer, J. *J. Phys. Chem.* **1997**, *B101*, 10035.
(12) Filippone, F.; Buda, F.; Iarlori, S.; Moretti, G.; Porta, P. *J. Phys. Chem.* **1995**, *99*, 12883.
(13) Nusterer, E.; Blöchl, P. E.; Schwarz, K. *Angew. Chem., Int. Ed. Engl.* **1996**, *35*, 175.
(14) Nusterer, E.; Blöchl, P. E.; Schwarz, K. *Chem. Phys. Lett.* **1996**, *253*, 448.
(15) Shah, R.; Payne, M. C.; Lee, M.-H.; Gale, J. D. *Science* **1996**, *271*, 1395.
(16) Haase, F.; Sauer, J.; Hutter, J. *Chem. Phys. Lett.* **1997**, *266*, 397.
(17) Schwarz, K.; Nusterer, E.; Margl, P.; Blöchl, P. E. *Int. J. Quantum Chem.* **1997**, *61*, 369.
(18) Shah, R.; Payne, M. C.; Gale, J. D. *Int. J. Quantum Chem.* **1997**, *61*, 393.
(19) Shah, R.; Gale, J. D.; Payne, M. C. *J. Phys. Chem.* **1997**, *B101*, 4787.
(20) Fois, E.; Gamba, A.; Tabacchi, G. *J. Phys. Chem.* **1998**, *B102*, 3974.
(21) Stich, I.; Gale, J. D.; Terakura, K.; Payne, M. C. *Chem. Phys. Lett.* **1998**, *283*, 402.
(22) Thomson, K. T.; Wentzcovitch, R. M.; McCormick, A.; Davis, H. T. *Chem. Phys. Lett.* **1998**, *283*, 39.
(23) Thomson, K. T.; Wentzcovitch, R. M. *J. Chem. Phys.* **1998**, *108*, 8584.
(24) Kessi, A.; Delley, B. *Int. J. Quantum Chem.* **1998**, *68*, 135.
(25) Termath, V.; Haase, F.; Sauer, J.; Hutter, J.; Parrinello, M. *J. Am. Chem. Soc.* **1998**, *120*, 8512.
(26) Jeanvoine, Y.; Ángyán, J. G.; Kresse, G.; Hafner, J. *J. Phys. Chem.* **1998**, *B102*, 5573.
(27) Jeanvoine, Y.; Ángyán, J. G.; Kresse, G.; Hafner, J. *J. Phys. Chem.* **1998**, *B102*, 7307.
(28) Civalleri, B.; Zicovich-Wilson, C. M.; Ugliengo, P.; Saunders, V. R.; Dovesi, R. *Chem. Phys. Lett.* **1998**, *292*, 394.
(29) Olson, D. H.; Dempsey, E. *J. Catal.* **1969**, *13*, 221.
(30) Vosko, S. H.; Wilk, L.; Nusair, M. *Can. J. Phys.* **1980**, *58*, 1200.
(31) Delley, B. *J. Chem. Phys.* **1990**, *92*, 508.
(32) Baker, J.; Andzelm, J.; Scheiner, A.; Delley, B. *J. Chem. Phys.* **1994**, *101*, 8894.
(33) Program DMol^3, version 3.5. Molecular Simulations Inc.: San Diego, CA, 1997.
(34) Perdew, J. P. *Physica* **1991**, *B172*, 1.
(35) Perdew, J. P. In *Electronic structure of solids*; Ziesche, P., Eschrig, H., Eds.; Akademie Verlag: Berlin, Germany, 1991.
(36) Mix, H.; Sauer, J.; Schröder, K.-P.; Merkel, A. *Coll. Czechoslovak Chem. Commun.* **1988**, *53*, 2191.
(37) Kazansky, V. B.; Gritscov, A. M.; Andreev, V. M.; Zhidomirov, G. M. *J. Mol. Catal.* **1978**, *4*, 135.
(38) Hill, J.-R.; Sauer, J. *J. Phys. Chem.* **1995**, *99*, 9536.
(39) Scheiner, A. C.; Baker, J.; Andzelm, J. W. *J. Comput. Chem.* **1997**, *18*, 775.
(40) Hirshfeld, F. L. *Theoret. Chim. Acta* **1977**, *44*, 129.
(41) Aprà, E.; Dovesi, R.; Freyria-Fava, C.; Pisani, C.; Roetti, C.; Saunders, V. R. *Modell. Simul. Mater. Sci. Eng.* **1993**, *1*, 297.
(42) Sauer, J.; Ugliengo, P.; Garrone, E.; Saunders, V. R. *Chem. Rev.* **1994**, *94*, 2095.
(43) Sauer, J. *J. Phys. Chem.* **1987**, *91*, 2315.
(44) Sauer, J. *Chem. Rev.* **1989**, *89*, 199.
(45) Beck, K.; Pfeifer, H.; Staudte, B. *Microporous Mater.* **1993**, *2*, 1.
(46) Fenzke, D.; Hunger, M.; Pfeifer, H. *J. Magn. Reson.* **1991**, *95*, 477.